Development 127, 5245-5252 (2000)
Printed in Great Britain © The Company of Biologists Limited 2000
DEV2606

Mesenchymal cells engulf and clear apoptotic footplate cells in macrophageless PU.1 null mouse embryos

William Wood[1], Mark Turmaine[1], Roberta Weber[1], Victoria Camp[1,2], Richard A. Maki[3,4], Scott R. McKercher[3] and Paul Martin[1,*]

[1]Department of Anatomy and Developmental Biology, University College London, Gower St, London WC1E 6BT, UK
[2]Institute of Laryngology and Otology, University College London, 330-332 Gray's Inn Road, London WC1X 8EE, UK
[3]The Burnham Institute, 10901 N. Torrey Pines Road, La Jolla, CA 92037, USA
[4]Neurocrine Biosciences, Inc., 3050 Science Park Rd., San Diego, CA 921211102, USA
*Author for correspondence (e-mail: paul.martin@ucl.ac.uk)

Accepted 13 October; published on WWW 14 November 2000

SUMMARY

Apoptosis is one of the key tools used by an embryo to regulate cell numbers and sculpt body shape. Although massive numbers of cells die during development, they are so rapidly phagocytosed that very few corpses are ever seen in most embryonic tissues. In this paper, we focus on the catastrophic cell death that occurs as the developing footplate is remodelled to transform webbed regions into free interdigital spaces. In the wild-type embryo, these dead cells are rapidly engulfed and cleared by macrophages. We show that in a macrophageless mouse embryo, null for the haemopoetic-lineage-specific transcription factor, PU.1, the task of phagocytosis is taken over by 'stand-in' mesenchymal neighbours in a clear example of cell redundancy. However, it takes three times as many of these mesenchymal phagocytes to complete the task and, at each stage of the clearance process – in the recognition of apoptotic debris, its engulfment and finally its digestion – they appear to be less efficient than macrophages. A molecular explanation for this may be that several of the engulfment genes expressed by macrophages, including the ABC1 transporter (believed to be part of the phagocytic machinery conserved from *Caenorhabditis elegans* to mouse), are not upregulated by these 'stand-in' phagocytes.

Key words: PU.1, Macrophages, Phagocytosis, Apoptosis, ABC-1, C1q, Mouse

INTRODUCTION

Programmed cell death is an important pattern-forming tool in embryonic development that is used to eliminate unwanted cells and to sculpt various tissues of the developing embryo (reviewed in Jacobson et al., 1997). The immediate fate of the dying cells is to be engulfed and cleared by neighbouring phagocytic cells, but while considerable efforts have been invested in understanding the intrinsic programmes that mediate cell death, less is known about the mechanisms of phagocytic recognition, engulfment and disposal of the resulting apoptotic debris. In amniote embryos, much of this debris is cleared by cells of the monocyte/macrophage lineage (Hume et al., 1983; Perry et al., 1985; Coudros et al., 1993; Hopkinson-Woolley et al., 1994). Studies in the mouse embryo using the lineage specific antibody, F4/80 (Austyn and Gordon, 1981) have shown that these cells first appear on about the tenth day of gestation in the yolk sac and liver; they then populate the spleen and invade surrounding mesenchymal tissues so that by mid-gestation most tissues have a resident population of macrophages (Morris et al., 1991).

We wanted to test the requirement for macrophages in the clearance of dead cells during vertebrate embryogenesis. To do this we have used a mouse genetically lacking macrophages. PU.1 (Sfpi1 – Mouse Genome Informatics) is an ETS family transcription factor that is expressed exclusively by cells of the haemopoetic lineage; a subset of these cells is missing in PU.1 null mice. They have no mature macrophages, osteoclasts, eosinophils or B cells; neutrophil development is retarded and aberrant; and T lymphocyte differentiation is delayed by up to two weeks (McKercher et al., 1996; Todravi et al., 1997; Anderson et al., 1998, McKercher et al., 1999). The only potential source of myeloid-derived phagocytes in these mice is a small pool of primitive 'macrophage-like' cells, expressing c-fms, but not F4/80 or any of the other established markers of macrophages, that may escape the PU.1 block and thus be present in the PU.1 null embryo (McKercher et al., 1996; Lichanska et al., 1999). PU.1 null mice are born alive but in the absence of neutrophils and macrophages are rapidly overcome by bacterial infection and die of septicaemia within 48 hours, unless they receive daily antibiotic injections.

One of the best characterised episodes of developmental cell death is in the developing footplate, where signals from the overlying limb epidermis trigger bone morphogenetic protein (BMP)-mediated, catastrophic and synchronous death of hundreds of interdigital mesenchymal cells, that will, after clearance, sculpt a separation between each of the toes (Hinchliffe, 1981; Garcia-Martinez et al., 1993, Rotello et al.,

1994; Zou and Niswander, 1996). The interdigit regions become heavily populated by macrophages and most of the dead cells are rapidly engulfed by these 'professional' phagocytes (Hopkinson-Woolley et al., 1994). We have studied the remodelling footplate in PU.1 null embryos and show that regression of interdigit web tissue is only slightly retarded, suggesting that compensatory mechanisms must be operating. In a clear example of cell redundancy, we demonstrate that neighbouring mesenchymal cells are able to take over the role of phagocytes, although it takes three times as many of them to complete the task as macrophages in a wild-type embryo.

It is now apparent that several components of the molecular machinery used by vertebrate macrophages to recognise and engulf apoptotic corpses are closely related to those needed for phagocytosis of dying cells in the worm *Caenorhabditis elegans* (reviewed in Savill, 1998; Platt et al 1998; Franc et al., 1999). Genetic studies in *C. elegans*, show that at least six genes, *ced-1, ced-2, ced-5, ced-6, ced-7* and *ced-10* regulate engulfment and digestion of cell debris (Ellis et al., 1991). Recently, a close homologue of ced-7, a murine ATP-binding cassette transporter, ABC1 (Abca1 – Mouse Genome Informatics), was shown to be specifically expressed by macrophages in regions of the embryo where active phagocytosis of apoptotic debris is taking place (Luciani and Chimini, 1996). ABC1 is apparently a key component of the macrophage recognition/engulfing machinery since in vitro antibody depletion experiments severely disable macrophage phagocytic capacity.

Clues as to other genetic components of the vertebrate phagocytosis repertoire come from various human diseases. For example, deficiency in the complement factor C1q in humans results in systemic lupus erythematosus (SLE) with resultant kidney damage caused by a failure to process and clear away immune complexes and apoptotic cells in the glomeruli (Walport and Morgan, 1991). C1q null mice also have diseased glomeruli containing large numbers of apoptotic bodies, suggesting that there is a deficiency in the clearance of apoptotic cells (Botto et al., 1998) The apparent connection between C1q deficiency and poor apoptotic cell clearance also led us to investigate the expression of C1q in interdigital cells of the embryonic mouse footplate.

Our observation that mesenchymal cells are able to stand in for macrophages in the PU.1 KO mouse would imply that these cells may adopt some of the molecular machinery normally used by macrophages to phagocytose dead cells. However, for the two 'engulfing' genes we have analysed here, this appears not to be the case. We show that while ABC1 and C1qa are both expressed by macrophages in the wild-type interdigit, neither gene is upregulated by mesenchymal 'stand-in' phagocytes in the PU.1 KO embryo.

MATERIALS AND METHODS

For this study we used the inbred mouse strain derived from D3jm p47 ES cells from the 129Sv strain, implanted into a C57 Bl/6 host and subsequently out-crossed onto a Black Swiss background, crossing male and female mice heterozygous for the targeted PU.1 mutation (McKercher et al., 1996). Midday on the day when a copulatory plug was first apparent was designated E0.5. Embryonic day 12.5, 13.5 and 14.5 progeny from such crosses were dissected from the uterus, and from their yolk sacs and amnions into PBS using watchmakers forceps. The yolk sac, and occasionally other tissues of the embryo such as the tail, were retained for subsequent PCR genotyping according to the protocol of McKercher et al (1996), using the PCR primers described therein.

Neonatal mice were PCR genotyped as above from tail tip samples. Blood smears were stained with Giemsa for rapid identification of null individuals, which have no neutrophils and an abundance of apoptotic debris in their blood (McKercher et al., 1996).

Scanning and transmission electron microscopy (SEM and TEM) and resin histology

Specimens for SEM, TEM or resin histology were first rinsed in PBS and fixed overnight in half strength Karnovsky fixative (Karnovsky, 1965) at 4°C. After fixation, forelimbs were dissected free of the trunk, rinsed in 0.1 M sodium cacodylate buffer, post-fixed in 1% osmium tetroxide in sodium cacodylate and further rinsed in 0.1 M sodium cacodylate buffer before being dehydrated through a graded ethanol series. Specimens for SEM were then critical-point dried in the standard way, and sputter coated with approximately 30 nm of gold before viewing on a Jeol 5410LV scanning electron microscope.

Specimens for resin histology were embedded in Araldite, sectioned at approximately 5 μm, and stained with Toluidine Blue. For examination by TEM, ultrathin Araldite sections were cut, stained with uranyl acetate and lead citrate, and examined using a Jeol 1010 transmission electron microscope.

Quantifying EM differences between PU.1 and wild-type embryos

SEM

In order to determine whether interdigit regression is hindered in PU.1 null embryos, we measured the mean interdigit regression angle for interdigit 2 at E12.5 and E13.5. This was done by taking the midpoint of the interdigit web and linking that point to the tips of digits 2 and 3 (see Fig. 1B). An average angle for the PU.1 null embryos from two litters was compared with the mean angle from all of their wild-type and heterozygous littermates at these stages.

TEM

We took sagittal EM sections at 50 μm intervals through the two interdigit spaces 1 and 2 (separating digits 1 and 2, and 2 and 3), and counted all apoptotic corpses and phagocytes in sample $50 \times 50\mu m$ grids in these sections. We also determined how many apoptotic cells still appeared 'free', i.e. not yet engulfed, or were in the act of being engulfed, by a phagocyte, and how many apoptotic cells/bodies were present within each phagocyte. Naturally, since these samples are two-dimensional, they do not represent absolute numbers of apoptotic bodies contained within each phagocyte but they do allow convenient comparison between E13.5 PU.1 null individuals and their wild-type littermates. We have also determined the stage of death and subsequent digestion of each apoptotic cell in these sections using four categories with the following criteria: (1) early stage dying cells, with peripheralised, condensed heterochromatin and dark cytoplasm, but still retaining patent nuclear and plasma membrane; (2) later stage apoptotic cells with more condensed nuclear heterochromatin and nuclear envelope now degenerated, with mitochondria and endoplasmic reticulum bloated or missing, and often with peripheral cytoplasmic vacuoles; (3) apoptotic bodies which are highly condensed heterochromatin spheres with little or no trace of peripheral cytoplasm; (4) apoptotic fragments or debris where the apoptotic body has become pale and moth-eaten. These categories and criteria are modified from older descriptions of the timecourse of apoptotic death in the regressing tadpole tail (e.g. Kerr et al., 1974), and all sections were assessed according to the same criteria by two of us, and a mean of our counts taken.

Acridine Orange

Embryonic forelimbs were removed and washed in PBS before being

incubated in 1 μg/ml Acridine Orange in PBS for 30 minutes at 37°C. Acridine Orange intensely stains chromatin-rich apoptotic bodies in living tissue (Graham, 1999). Specimens were then rinsed twice for 5 minutes in PBS before being mounted in PBS and viewed and photographed under a Leica MZFLIII fluorescent dissecting scope.

F4/80 immunostaining

Embryos were fixed overnight in 4% paraformaldehyde in PBS at 4°C, dehydrated through a graded series of ethanols and embedded in wax. Sections of 5 μm were cut and mounted on Tespa (Sigma)-coated slides. To stain for macrophages the sections were first rehydrated, rinsed in PBS and then soaked in 0.3% H_2O_2 in methanol for 40 minutes, in order to block endogenous peroxidase activity. After further PBS washes the sections were treated with rabbit serum at a concentration of 1:100 to block nonspecific binding of the antibody. The footplate sections were then incubated overnight at 4°C with the macrophage specific, rat anti-mouse monoclonal antibody, F4/80 (Austyn and Gordon 1981) at a concentration of 8.5 μg/ml. After further washes in PBS, bound antibody was detected using biotinylated anti-rat IgG (made in rabbit and mouse adsorbed) and the avidin-biotin-peroxidase complex. To detect the peroxidase activity a diaminobenzidine tetrahydrochloride (DAB) kit was used as directed by the manufacturer's instructions (Vector Laboratories). The sections were then washed in tap water and counterstained with Mayer's Haemalum before being dehydrated through graded ethanols and mounted in XAM (Sigma).

Whole-mount in situ hybridisation

Embryonic forelimbs were removed and fixed in 4% paraformaldehyde in PBS overnight at 4°C. Hybridisations were performed according to the protocol of Shamim et al (1999). Digoxigenin (DIG) labelled riboprobes were generated from a 1450 bp cDNA fragment of murine ABC1 (courtesy of Giovanna Chimini, Inserm CNRS, Marseille), and a 540 bp cDNA fragment of murine C1qa (courtesy of Marina Botto, Hammersmith Hospital, London). Bound probe was detected using an anti-DIG alkaline phosphatase-conjugated antibody (Boehringer Mannheim), and the antibody was visualised with NBT and BCIP. The specimens were then washed thoroughly in PTW (PBS + 0.02M EDTA in 0.1% Tween-20) and refixed in 4% paraformaldehyde prior to photography.

RESULTS

Macrophages are the prime phagocytes of interdigital apoptosis in the mouse footplate

Between embryonic days E12.5 and E14.5, the mouse forelimb footplate is sculpted from a paddle-shaped block into a miniature model of the adult foot, with five separated toes. A series of scanning electron microscope views during this period shows how the interdigital webbing regresses as the digits extend (Fig. 1A-C). Much of this remodelling is achieved through the death of interdigital mesenchymal cells and their subsequent clearance by macrophages. Resin histology and Acridine Orange staining of whole-mount preparations both revealed a trickle of cells beginning to die from about E12.5 in the peripheral interdigital margins (Fig. 2A-D,F). The peak of cell death appeared to be at about E13.5 (Fig. 2D), and from then on, the numbers of apoptotic cells tailed off until about E14.5 when Acridine Orange staining was restricted only to a small number of cells lining the remaining clefts and lateral edges of each digit (Fig. 2C). To investigate the role of macrophages in clearance of this apoptotic debris we have stained with the monocyte/macrophage specific antibody F4/80 (Austyn and Gordon, 1981). This antibody revealed large numbers of macrophages in the death zones throughout the remodelling period (Fig. 3A-C). Many of these 'professional' phagocytes are swollen with apoptotic corpses, suggesting that most, if not all, of the dead cells were being engulfed by F4/80 positive phagocytes (Fig. 3D,E).

TEM views of the regressing E13.5 interdigit at the time of the peak cell death period showed numerous characteristic macrophages, each containing the remnants of up to 10 (or occasionally more) apoptotic bodies (Fig. 4A). We found only a minimal number of free apoptotic corpses that had yet to be engulfed and all of these were at the earliest morphological stage of apoptosis, suggesting that recognition and engulfment of a dying cell must be rapid and occur early on in the death programme. In addition to macrophages, we also saw small numbers of phagocytes adjacent to the regressing epidermal webbing, which contained only one or two corpses and may have been opportunistic mesenchymal cells that had phagocytosed a dead cell before the nearest macrophage could get to it (Fig. 4B).

Interdigit regression is scarcely retarded in the macrophageless PU.1 KO mouse embryo

PU.1 null forelimb footplates were first stained with the macrophage-specific antibody F4/80 to confirm absence of the monocyte/macrophage lineage (Fig. 3F). In order to examine the gross effects of macrophage absence on limb remodelling, we analysed web regression in PU.1 null versus wild-type embryos by calculating the mean interdigit regression angles of interdigit 2 (between digits 2 and 3 – see Fig. 1B) at various stages during footplate remodelling. Our data show that although regression does proceed in macrophageless embryos, it is slightly but significantly retarded. As expected, at E12.5, prior to when regression commences, embryonic footplates looked identical in wild-type and PU.1 null embryos (Fig. 1A,D). However, by E13.5 a slight retardation in regression is seen in the PU.1 null embryos, with a regression angle of 137°±1.9° (mean±s.e.m.; n=7), by comparison with 126°±1.6° (mean±s.e.m.; n=13) in heterozygote and wild-type sibling embryos (Fig. 1B,E).

By E14.5, even given stage variation within a litter, we can very accurately stage-match individual wild-type embryos with equivalent stage PU.1 null embryos without recourse to footplate shape. At this stage, hair buds are beginning to develop on the dorsal aspect of the forelimb and their distribution provides a continually evolving marker of the precise developmental age. This comparison reveals that web regression in the PU.1 null footplates completely catches up with that in wild-type embryos by E14.5 (Fig. 1C,F).

In the absence of macrophages, mesenchymal neighbours phagocytose the interdigital apoptotic corpses

Acridine Orange staining and resin histology of PU.1 null footplates during the period of normal remodelling revealed that, while the time of onset of cell death was similar to that in wild-type embryos, the distribution of dead cells in each interdigit was very different. In wild-type embryos the dead cells were clearly packaged together into separate small aggregates, presumably reflecting their confinement within individual macrophages (Fig. 2D,F). By contrast, in PU.1 null footplates the apoptotic foci were not in aggregates but were

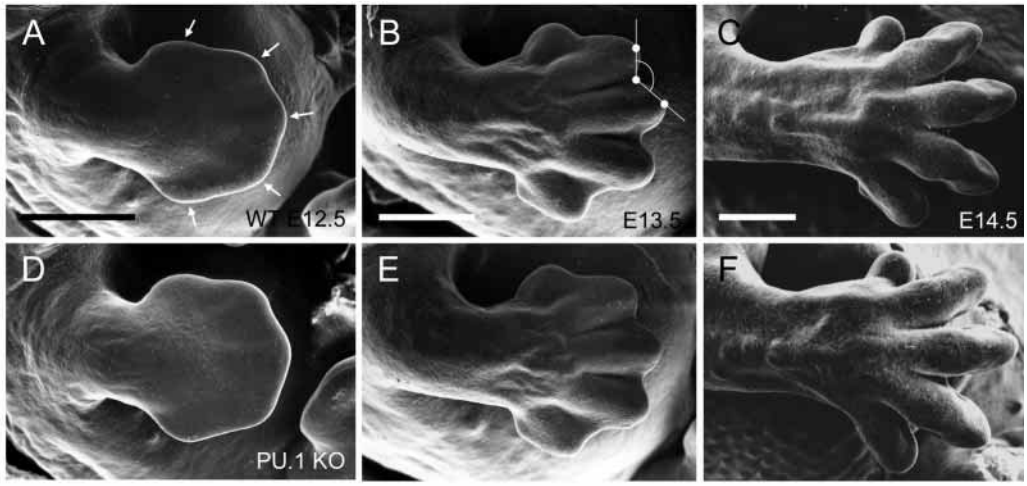

Fig. 1. Scanning electron microscope (SEM) series of wild-type (A-C) and PU.1 null embryo (D-F) remodelling forelimb. (A) At E12.5. the wild-type forelimb footplate appears corrugated with the ridges (arrows) corresponding to where digits 1-5 will form (1 being the most anterior). (B) One day later at E13.5, the interdigital webs are beginning to regress ('regression angle' of interdigit 2 indicated by white lines). (C) By E14.5, web regression is almost complete. (D) At E12.5 the PU.1 null footplate is indistinguishable from its wild-type counterpart, above. (E) By E13.5 the PU.1 footplate appears slightly retarded in its degree of web regression. (F) By E14.5 this slow regression seems to have caught up with the wild type such that it is again indistinguishable from the wild-type footplate shown in C. Scale bars: 500 μm.

evenly spread throughout the interdigit (Fig. 2G,I). Precisely the same difference in spatial distribution of apoptotic debris was seen in PU.1 null versus wild-type embryos in the zone of cell death in the fused ventral aspect of the genital tubercle (Fig. 2E,H), suggesting that this is a universal phenomena.

At the TEM level, we found no cells with the classic morphology of a macrophage in the PU.1 null footplate. Rather, at E13.5, when cell death was at its peak, the vast majority of apoptotic nuclei appeared to have been engulfed instead by healthy mesenchymal neighbours that are also within the web region (Fig. 4C). Most of these stand-in phagocytes contain the remains of only one or two cells. In wild-type embryos we seldom captured the moment of engulfment by a macrophage, but in PU.1 null embryos we saw many examples of healthy cells spreading around an adjacent apoptotic cell, as though in the process of engulfing it (Fig. 4 C,D), suggesting that engulfment may be a slower process than in macrophages. In the PU.1 null footplate we saw small, but significant numbers of 'free' apoptotic cells (Fig. 4D), suggesting that "stand-in" mesenchymal phagocytes may also be somewhat slower or less efficient at recognising apoptotic debris.

In an attempt to quantify these differences in the efficiency of recognition, engulfment and also of digestion, we calculated the density of phagocytes within the interdigit death zones, the numbers of 'free' apoptotic corpses and the mean number of corpses per phagocyte, and assessed the digestion profile of the engulfed corpses, for wild-type and for PU.1 null embryos. The mean density of phagocytes (largely macrophages) from sample sections of interdigits 1 and 2 in wild-type embryos was 8.1±1.0/2500 μm^2 (mean±s.e.m., n=16), while in equivalent PU.1 null sections, the density tripled to 25.2±1.6 phagocytes/2500 μm^2 (n=14). In some PU.1 null sample grids,

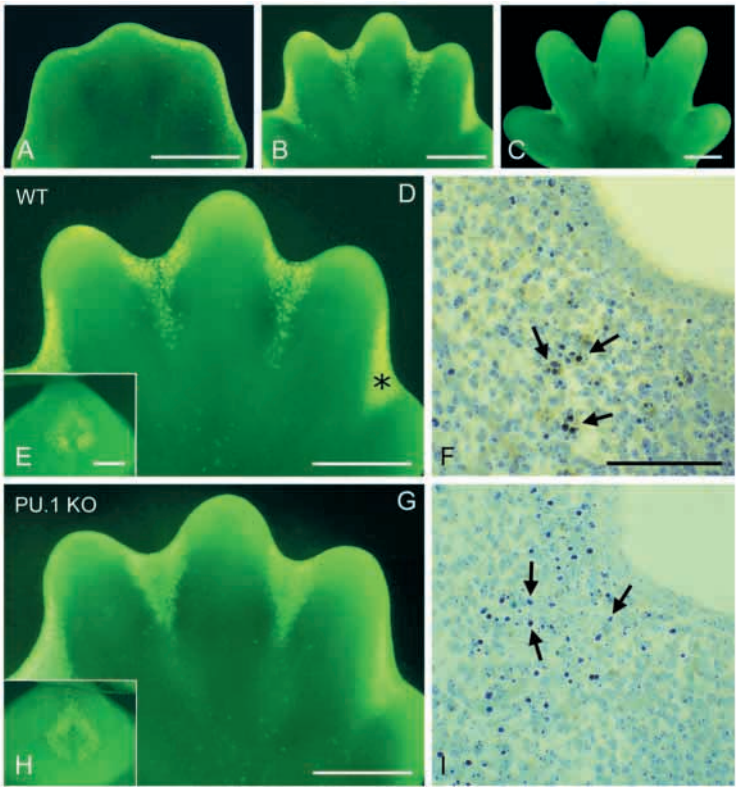

Fig. 2. Acridine Orange and resin histology to reveal cell death distribution in wild-type (A-F) and PU.1 null (G,I) footplates. Acridine Orange staining of wild-type whole-mount footplates reveals cell death first apparent in the interdigit margins at E12.5 (A). Numbers of dying cells peak in the interdigit at E13.5 (B) and have diminished to small numbers at the web base and lateral margins of each digit by E14.5 (C). D shows a high magnification detail of B and reveals that dead cells appear clustered in small aggregates within the interdigit zone. (E) A similar 'aggregated' distribution of dead cells on the ventral aspect of the wild-type genital tubercle. (F) Resin section of the interdigit zone asterisked in D. The Acridine Orange aggregates represent packets of three or more apoptotic bodies presumably encapsulated within one macrophage (arrows). Acridine Orange staining of the PU.1 KO embryo reveals a more diffuse staining of dead cells in the footplate (G) and genital tubercle (H), which is mirrored by dispersed apoptotic nuclei in a resin section through the footplate web region (arrow in I). Scale bars: A-D,G, 250μm; E,H and F,I, 100 μm.

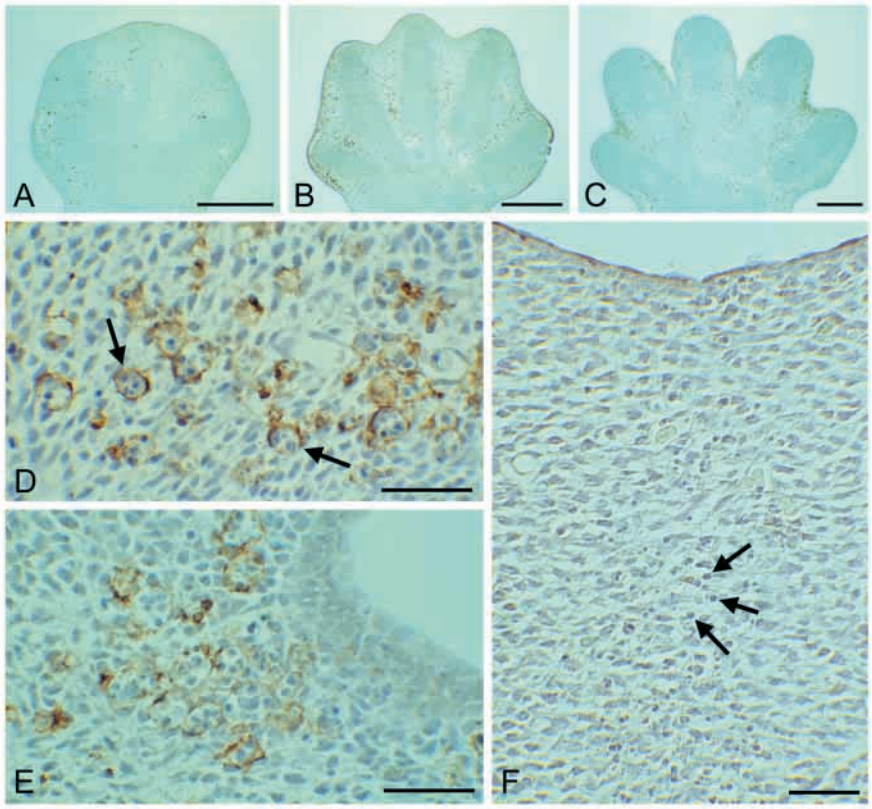

Fig. 3. F4/80 immunostaining of monocytes and macrophages in the wild-type (A-E) and PU.1 null (F) footplate. Small numbers of brown staining macrophages are seen in the wild-type footplate at E12.5 (A) when the first dead cells are apparent. At E13.5, the interdigits are crowded with F4/80 positive cells (B), but by E14.5 numbers of macrophages have diminished and are restricted to the sites where dying cells still persist along the margins of each digit (C). D is a high magnification detail from B showing the density of macrophages in the core of the interdigit; note that each macrophage (arrows, delineated by its brown staining plasma membrane) contains several darkly staining apoptotic corpses. (E) A high magnification detail from C reveals that although there are fewer macrophages in the E14.5 footplate, they are, if anything, even more laden with dead cells than a day earlier. (F) F4/80 immunostaining of an E13.5 PU.1 interdigit reveals dark staining apoptotic cells (arrows) but no trace of any F4/80 positive monocytes or macrophages. Scale bars: A-C, 250 μm; D-F, 50 μm.

almost every healthy cell contained at least one apoptotic corpse. The mean number of apoptotic corpses per phagocyte was 4.5 in the wild-type embryo but only 1.5 for PU.1 null mesenchymal phagocytes. These data suggest that similar total numbers of apoptotic corpses are phagocytosed in PU.1 null, by comparison with wild type, footplates, but that this cell death clearance is achieved by three times as many phagocytes engulfing, on average, a third as many corpses per phagocyte as their wild-type counterparts. We observed less than one 'free' apoptotic corpse/10000 μm^2 in the wild-type footplate, and those that we found were at the earliest recognisable stage of cell death with membranes still intact and healthy looking mitochondria. However, in PU.1 null interdigits, a mean of 11 apoptotic corpses/10000 μm^2 (6.7% of all apoptotic corpses counted) was still unengulfed. Some of these cell corpses were at an advanced stage of apoptosis, with their nuclear envelope missing and with degenerating organelles (Fig. 4D). Finally, using a score of 1-4, with 4 being the most advanced/digested state of apoptotic debris (see Materials and Methods for fuller criteria), we determined the digestion profile of apoptotic cells within wild-type macrophages versus PU.1 null phagocytes. As a measure of digestion efficiency we compared the ratio of category 3 corpses (condensed apoptotic bodies) with those

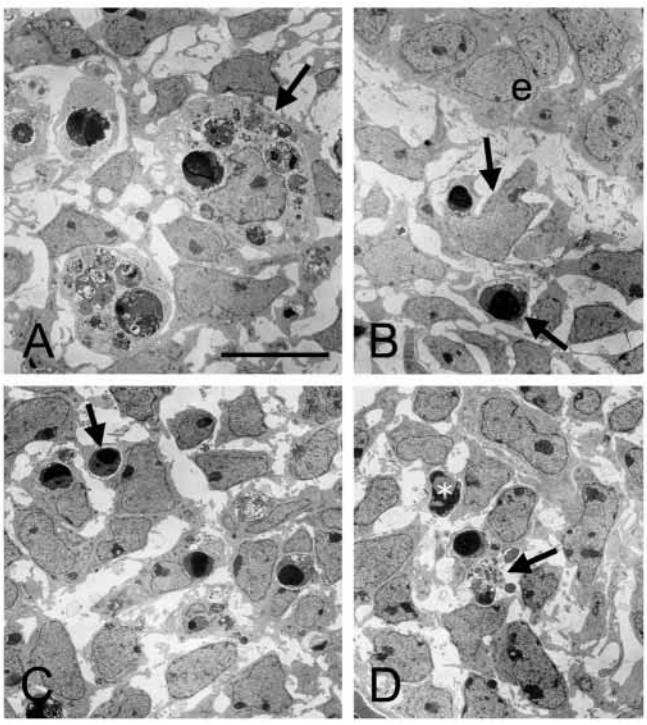

Fig. 4. Transmission electron microscopy (TEM) to reveal apoptotic debris and phagocytes in wild-type and PU.1 null interdigits. (A) A typical macrophage (arrow) in the wild-type interdigit; each macrophage contains up to 10 or more apoptotic corpses. (B) Close to the regressing epithelium (e) in the wild-type footplate we observe phagocytes containing only one or two apoptotic corpses (arrows). (C) In the PU.1 null footplate there are larger numbers of mesenchymal phagocytes each containing only one or two (or occasionally more) apoptotic corpses. Fairly frequently we capture these PU.1 stand-in phagocytes in the act of engulfing an apoptotic neighbour (arrow). (D) Often we observe more than one PU.1 null mesenchymal phagocyte competing for the same apoptotic corpse (asterisk), but there are also significant numbers of 'free' corpses as yet not recognised or engulfed by the PU.1 null stand-in phagocytes (arrow). Scale bar: 10 μm.

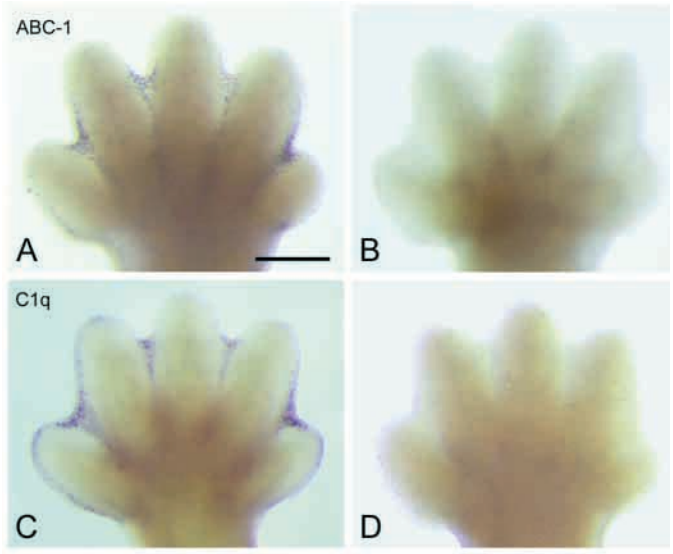

Fig. 5. Whole-mount digoxigenin in situ studies of engulfing genes in wild-type (A,C) and PU.1 null (B,D) E13.5 footplates. (A) Bright expression (purple staining) of ABC1 mRNA in the interdigital macrophages of an E13.5 wild-type embryo. (B) A PU.1 null sibling embryo shows no such expression. (C) Similarly, C1qa expression is restricted to the macrophage clearance domains in a wild-type footplate, but is absent in a PU.1 null sib footplate (D). Scale bar: 250 μm.

assessed as category 4 (apoptotic fragments) in order to quantify efficiency of intracellular conversion of category 3 into category 4 corpses. In wild-type macrophages the mean ratio was 1:2, while in PU.1 null footplates it was only 1:1.5 suggesting that PU.1 null mesenchymal phagocytes are also slower at digesting apoptotic corpses than are macrophages in wild-type embryos.

Phagocytic mesenchymal cells fail to upregulate two of the macrophage 'engulfing' genes

Phagocytosis is a specialist cell function requiring expression of various 'engulfing' genes, some of which may have conserved function from *C. elegans* to mouse (reviewed in Savill, 1998; Platt et al., 1998; Franc et al., 1999). We have set out to test whether a selection of this genetic portfolio of phagocytosis tools is used by stand-in phagocytes in the PU.1 KO mouse. Whole-mount in situ hybridisation studies to investigate the expression of the ced-7 homologue, ABC1, confirm previous studies by Luciani et al. (1996) and show it to be expressed by macrophages in the wild-type interdigit (Fig. 5A). However, although mesenchymal neighbours are able to engulf and clear away apoptotic corpses in the PU.1 KO footplate, we find that ABC1 is not expressed by these cells at any stage during the remodelling phase (Fig. 5B). Clearly, in higher vertebrates this gene is macrophage specific and is not switched on by other cells when they stand-in as replacement phagocytes.

We also investigated the expression of a non-ced 'engulfing' gene, the complement component factor, *C1qa*, in the developing mouse footplate. This gene, like ABC1, is robustly expressed by macrophages in the interdigit at a stage when they are actively engulfing apoptotic cells (Fig. 5C), but again, in the PU.1 KO mouse *C1qa* is not expressed by 'stand-in' mesenchymal phagocytes (Fig. 5D).

DISCUSSION

In this paper we analyse the relationship between macrophages and programmed cell death during sculpting of the mouse embryo footplate and compare interdigit regression in wild-type versus PU.1 knockout embryos that have no macrophages. One clear observation we make is that there are almost equivalent numbers of dying cells in the PU.1 KO footplate suggesting that in this region of the embryo, at least, macrophages are not the essential triggers of the apoptotic programme that they appear to be for some populations of dying cells, for example, those in the developing eye (Lang and Bishop, 1993; Diez-Roux and Lang, 1997).

In the wild-type embryo, macrophages appear to be responsible for almost all the clearance of the footplate apoptotic debris, but we show here how neighbouring mesenchymal cells in the macrophageless PU.1 null embryo are also competent to act as stand-in phagocytes. At the macroscopic level, it appears that clearance and regression of interdigital tissue occurs almost as efficiently in PU.1 null embryos as in their wild-type sibs, and at the cell level we see large numbers of mesenchymal cells actively engulfing apoptotic debris. This dramatic example of cell redundancy in the embryo raises several questions: first, are mesenchymal cells in wild-type embryos able to clear away cell death, and do they? And second, how does a mesenchymal cell undertake to 'stand-in' as a phagocyte – does it use the same genetic phagocytic machinery as a macrophage, or just a small subset of that machinery, or does it use alternative strategies entirely?

Our TEM data suggests that individual neighbouring PU.1 null mesenchymal cells are slower at both recognising and engulfing apoptotic debris than macrophages in the wild-type interdigit. This we presume from the fact that more than occasional free apoptotic bodies are seen in the PU.1 null footplate and that we see many examples of PU.1 null phagocytes in the act of engulfing a dead neighbour. This inefficiency in recognition and engulfment is apparently compensated for by greater numbers of mesenchymal phagocytes in the PU.1 null footplate than macrophages in the wild-type footplate, such that interdigit regression is barely slowed down. These larger numbers of stand-in phagocytes (about three times as many as macrophages) contain on average a third as many apoptotic corpses as their professional counterparts in the wild-type footplate (Fig. 4). Also significant is the profile of digestion state of the apoptotic bodies contained within PU.1 null stand-in phagocytes, by comparison with the apoptotic debris observed within their wild-type macrophage counterparts. Macrophages engulf apoptotic cells at an earlier stage in the death programme than PU.1 stand-in phagocytes and yet the digestion profile of their prey is more advanced, suggesting that the stand-in phagocytes may not only be less efficient at recognition and capture of apoptotic cells but also slower at digesting them once engulfed.

Almost certainly, mesenchymal cells in wild-type embryos are capable of participating in clearance of the large numbers of dead cells in the interdigit, but they simply get very little opportunity to perform because the more motile and observant macrophages engage and mop up almost all the dead cells so rapidly. In fact, there do seem to be occasional examples in the wild-type footplate of morphological mesenchymal cells that have engulfed a dead cell or two; these examples are largely

adjacent to the regressing interdigit epithelium, which is perhaps a site where macrophages are at less of an advantage over neighbouring mesenchymal cells because of poor access. Indeed, the very occasional free apoptotic cells that we do find in the wild-type footplate are always located close to the regressing epithelium. Certainly, at earlier stages of embryogenesis, before the monocyte lineage has begun to differentiate, there are several occasions when significant numbers of cells die by programmed cell death, for example, during cavitation of the egg cylinder (Coucouvanis and Martin, 1995), and at the seam of the closing neural tube (Weil et al., 1997). There are some data to show that neighbouring, non-monocyte derived cells might be capable of engulfing their neighbours in these early stage examples of apoptotic tissue remodelling (El-Shershaby and Hinchliffe, 1974; Hardy et al., 1996). After monocyte lineages are established in the embryo there are several locations where their numbers remain extremely sparse, for example, in germinal layers containing proliferating neuroblasts in regions of the CNS such as the external granule layer of the cerebellum (Ashwell, 1990). Again, neighbouring cells, in this case astrocytes, may play a major role in cell death clearance, given more of a spatial advantage over the competing monocyte-derived microglia (Parnaik et al., 2000).

In order to act as 'stand-in' phagocytes in the PU.1 embryo, mesenchymal cells must either use a set of recognition, engulfment and digestion genes that are universal to all cells, or perhaps, upregulate a battery of genes especially for the job. These engulfing genes may be a subset of those that form part of the normal portfolio of the wild-type macrophage, or a set of genes that allow an alternative mode of phagocytosis. We have gone some way to addressing this question by analysing expression of ABC1, which seems likely to be a vertebrate homologue of the *C. elegans* gene, *ced-7*, and so part of an ancient family of phagocytosis genes, conserved from before the time when macrophages evolved. Surprisingly, although ABC1 is expressed by macrophages in the wild-type footplate and is apparently required by macrophages to engulf dead cells (Luciani and Chimini, 1996), it is not expressed in the PU.1 null footplate. Clearly, while ced-7 is used by non-professional phagocytes in *C. elegans* in order to clear dead neighbours (Wu and Horvitz, 1998), its equivalent in higher vertebrates is macrophage specific and is not switched on by other cells when they stand-in as replacement phagocytes. We have looked at one other potential 'engulfing' gene that encodes the C1qa component of the complement system. *C1qa* null mice show a reduced capacity to clear dead cells (Botto et al., 1999), and we show that *C1qa* is specifically expressed by interdigital macrophages in the wild-type mouse, but again, in the PU.1 null mouse this 'engulfing' gene is not upregulated by 'stand-in' mesenchymal cells.

It may be that the two genes we have looked at are part of the rapid recognition apparatus which allows macrophages to 'see' dead cells early in the death programme, and so might be a part of the molecular explanation for why PU.1 null mesenchymal phagocytes are slower than wild-type macrophages and why macrophages generally 'beat mesenchymal cells to the draw' in wild-type embryos. Still, the question remains: what might be the molecular basis of non-macrophage phagocytosis, and it seems likely that the PU.1 KO mouse will be an excellent in vivo model in which to find this out.

Of some relevance is the observation by Caron and Hall (1998), that macrophage engulfment of particles coated either by antibodies or complement are not only recognised by two separate receptors but are drawn into the same phagocyte by entirely different actin- and membrane-driven processes, one mediated by the small GTPase molecular switch Rho, and the other by Rac and Cdc42. It may be that fibroblast phagocytes recognise different, possibly later expressed, epitopes on dead cells than do macrophages, and thus activate entirely different engulfing mechanisms. This alternative route may or may not also be available to macrophages. Investigations of macrophage clearance capacity in the footplates of ABC1 and *C1qa*-null mice will be interesting in this regard. Certainly, it appears that phagocytic clearance of apoptotic debris is so crucial a process during embryonic and adult life that several redundant genetic pathways and cell lineages can partake in this mopping-up operation, and the remodelling footplate may prove to be an ideal in vivo system in which to analyse these various clearance strategies.

We thank Siamon Gordon (Oxford) for F4/80 antibody, and Giovanna Chimini (Marseille) and Marina Botto (London) for generously supplying us with appropriate plasmids for ABC1 and C1qa in situs, respectively. We also greatly appreciate the constant helpful advice and guidance from Siamon Gordon and John Scholes in all things related to macrophages and phagocytotosis, and are indebted to John Scholes for very useful criticisms of drafts of this manuscript. Finally, P. M. thanks the Wellcome Trust, Pfizer UK and the MRC, for funding the project.

REFERENCES

Anderson, K. L., Smith, K. A., Conners, K., McKercher, S. R., Maki, R. A. and Torbert B. E. (1998). Myeloid development is selectively disrupted in PU.1 null mice. *Blood* **91**, 3702-3710.

Ashwell, K. (1990). Microglia and cell death in the developing mouse cerebellum. *Dev. Brain Res.* **55**, 219-230.

Austyn, J. M. and Gordon, S. (1981). F4/80, a monoclonal antibody directed specifically against the mouse macrophage. *Eur. J. Immunol.* **11**, 805-915.

Botto, M., Dell'Agnola, C., Bygrave, A. E., Thompson, E. M., Cook, H. T., Petry, F., Loos, M., Pandolfi, P. P. and Walport, M. J. (1998). Homozygous C1q deficiency causes glomerulonephritis associated with multiple apoptotic bodies. *Nat. Genet.* **19**, 56-59.

Caron, E. and Hall, A. (1998). Identification of two distinct mechanisms of phagocytosis controlled by different Rho GTPases. *Science* **282**, 1717-1721.

Coucouvanis, E. and Martin, G. R. (1995). Signals for death and survival: a two step mechanism for cavitation in the vertebrate embryo. *Cell* **83**, 279-287.

Coudros, M. E., Martin, C., Coltey, P., Almendros, A. and Navascues, J. (1993). First appearance, distribution, and origin of macrophages in the early development of the avian central nervous system. *J. Comp. Neurol.* **330**, 113-129.

Diez-Roux, G. and Lang, R. A. (1997). Macrophages induce apoptosis in normal cells in vivo. *Development* **124**, 3633-3638.

Ellis, R. E., Jacobson, D. M. and Horvitz, H. R. (1991). Genes required for the engulfment of cell corpses during programmed cell death in Caenorhabditis elegans. *Genetics* **129**, 79-94.

El-Shershaby, A. M. and Hinchliffe, J. R. (1974). Cell redundancy in the zona-intact preimplantation mouse blastocyst: a light and electron microscope study of dead cells and their fate. *J. Embryol. Exp. Morphol.* **31**, 643-654.

Franc, N. C., White, K. and Ezekowitz, R. A. B. (1999). Phagocytosis and development: back to the future. *Curr. Opin. Immunol.* **11**, 47-52.

Garcia-Martinez, V., Macias, D., Ganan, Y., Garcia-Lobo, J. M., Francia, M. V., Fernandez-Teran, M. A. and Hurle, J. M. (1993). Internucleosomal DNA fragmentation and programmed cell death (apoptosis) in the interdigital tissue of the embryonic chick leg bud. *J. Cell Sci.* **106**, 201-208.

Graham. A. (1999). Whole embryo assays for programmed cell death. *Methods Mol. Biol.* **97**, 667-672.

Hardy, K., Warner, A., Winston, R. M. and Becker, D. L. (1996). Expression of intercellular junctions during pre-implantation development of the human embryo. *Mol. Hum. Reprod.* **2**, 621-632.

Hinchliffe, J. R. (1981). Cell death in embryogenesis. In *Cell Death in Biology and Pathology*. (ed. I. D. Bowen and R. A. Lockshin), pp. 35-69. London: Chapman and Hall.

Hopkinson-Woolley, J., Hughes, D., Gordon, S. and Martin, P. (1994). Macrophage recruitment during limb development and wound healing in the embryonic and foetal mouse. *J. Cell. Sci.* **107**, 1159-1167.

Hume DA, Perry, V. H. and Gordon, S. (1983). Immunohistochemical localisation of macrophage-specific antigen in the developing mouse retina: Phagocytosis of dying neurones and differentiation of microglial cells to form a regular array in the plexiform layers. *J. Cell Biol*. **97**, 253-257.

Jacobson, M. D., Weil, M. and Raff, M. C. (1997). Programmed cell death in animal development. *Cell* **88**, 347-354.

Karnovsky, M. J. (1965) A formaldehyde-gluteraldehyde fix of high osmolarity for use in electron microscopy. *J. Cell Biol.* **27**, 137-138.

Kerr, J. F., Harmon, B. and Searle, J. (1974). An electron-microscope study of cell deletion in the anuran tadpole tail during spontaneous metamorphosis with special reference to apoptosis of striated muscle fibers. *J. Cell Sci.* **14**, 571-585.

Lang, R. A. and Bishop, M. J. (1993). Macrophages are required for cell death and tissue remodelling in the developing mouse eye. *Cell* **74**, 453-462.

Lichanska, A. M., Browne, C. M., Henkel, G. W., Murphy, K. M., Ostrowski, M. C., McKercher, S. R., Maki, R. A. and Hume, D. A. (1999). Differentiation of the mononuclear phagocyte system during mouse embryogenesis: the role of transcription factor PU.1. *Blood* **94**, 127-138.

Luciani, M-F. and Chimini, G. (1996). The ATP binding cassette transporter ABC1, is required for the engulfment of corpses generated by apoptotic cell death. *EMBO J.* **15**, 226-235.

McKercher, S. R., Torbert, B. E., Anderson, K. L., Henkel., G. W., Vestal, D. J., Baribault, H., Klemsz, M., Feeney, A. J., Wu, G. E. et al. (1996). Targetted disruption of the PU.1 gene results in multiple hematopoietic abnormalities. *EMBO J.* **15**, 5647-5658.

McKercher, S. R., Henkel, G. W. and Maki, R. A. (1999). The transcription factor PU.1 does not regulate lineage commitment but has lineage-specific effects. *J. Leukoc. Biol.* **66**, 727-732.

Morris L, Graham, C. F. and Gordon S. (1991). Macrophages in haemopoietic and other tissues of the developing mouse detected by the monoclonal antibody F4/80. *Development* **112**, 517-526.

Parnaik, R., Raff, M and Scholes J. (2000). Differences between the clearance of apoptotic cells by professional and non-professional phagocytes. *Curr. Biol*. **10**, 857-860.

Perry, V. H., Hume, D. A. and Gordon, S. (1985). Immunocytochemical localization of macrophages and microglia in the adult and developing mouse brain. *Neuroscience* **15**, 313-326.

Platt, N., da Silva, R. P. and Gordon, S. (1998). Recognising death: the phagocytosis of apoptotic cells. *Trends Cell Biol*. **8**, 365-372.

Rotello, R. J., Fernandez, P-A and Yuan, J. (1994). Anti-apogens and anti-engulfens: monoclonal antibodies reveal specific antigens on apoptotic and engulfment cells during chicken embryonic development. *Development* **120**, 1421-1431.

Savill, J. (1998). Phagocytic docking without shocking. *Nature* **392**, 442-443.

Shamim, H., Mahmood, R. and Mason, I. (1999). In situ hybridization to RNA in whole embryos. *Methods Mol. Biol.* **97**, 623-633.

Tondravi, M. M., McKercher, S. R., Anderson, K., Erdmann, J. M., Quiroz, M., Maki, R. A. and Teitelbaum, S. L. (1997). Osteopetrosis in mice lacking haematopoietic transcription factor PU.1. *Nature* **385**, 81-84.

Walport, M. J. and Morgan, B. P. (1991). Complement deficiency and disease. *Immunol. Today* **12**, 301-306.

Weil, M., Jacobson, M. D. and Raff, M. C. (1997). Is programmed cell death required for neural tube closure? *Curr. Biol*. **7**, 281-284.

Wu, Y. C. and Horvitz, H. R. (1998). The C. elegans cell corpse engulfment gene ced-7 encodes a protein similar to ABC transporters. *Cell* **93**, 951-960.

Zou, H. and Niswander, L. (1996). Requirement for BMP signaling in interdigital apoptosis and scale formation. *Science* **272**, 738-741.